

CHAPTER FIFTY SEVEN

Model Harbour Seiching Compared to Prototype Data

W A M Botes*, K S Russell*, P Huizinga*

1. INTRODUCTION

Since 1978 a finite-difference numerical model based on that developed by Leendertse and adapted for resonance studies (Russell and Huizinga, 1978) has been applied to investigate harbour resonance in Table Bay Harbour and several other South African ports.

During April 1981 three long-wave recorders were installed in the cooling water intake basin of the Koeberg Nuclear Power Station to determine the occurrence and magnitude of the long waves and to measure the corresponding response of the basin. Koeberg is situated on the west coast of South Africa, 30 km north of Cape Town and is exposed to the approaching cyclonic weather systems which experience has shown to be associated with the occurrence of long waves. An example of an approaching low pressure system with the location of Koeberg is shown in figure 1.

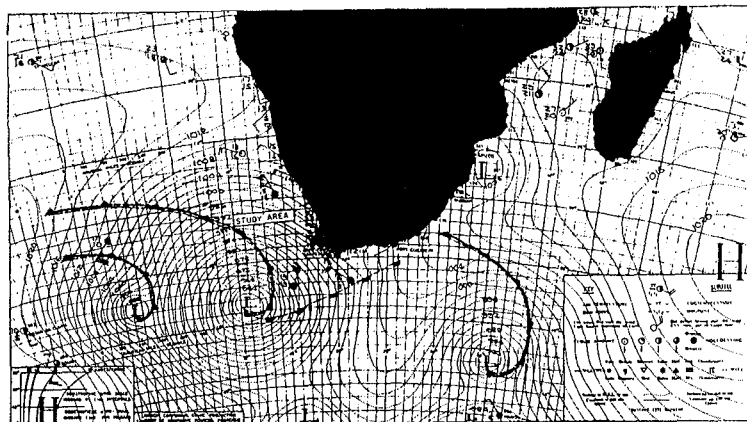


Figure 1. South Africa with approaching low-pressure systems, passing from west to east

Data were sampled over a period of two years and a paper on the characteristics of the long waves in the Koeberg basin was presented at the ICCE in 1982 by Botes, Russell and Huizinga (1982). In that paper the

* National Research Institute for Oceanology, Stellenbosch, Republic of South Africa.

correlation between the occurrence of long-period waves and short-period waves was shown. During the sample period the recorders were switched to continuous mode during extreme weather conditions. These relatively long records could be analysed with a high degree of confidence and resolution for determining the response of the basin.

This paper presents further work using prototype results since they provide the basic data to calibrate and verify a numerical model of the Koeberg basin designed to study its resonance characteristics. This also allowed the investigation of aspects such as the sensitivity of the numerical model to grid sizes, computational time steps, friction, etc. The Koeberg intake basin provides an ideal configuration for the abovementioned investigations, as the basin is of medium size and situated on a straight coastline with a uniformly contoured seabed.

2. PROTOTYPE DATA SAMPLING

The water level recorders used consist of pressure transducers connected to magnetic tape recorders. Data were sampled at an interval of 1,0 s for a duration of 50 minutes every 12 hours. When resonance was visually observed the recorders were switched to continuous mode.

Three water-level recorders were installed in the basin and were in operation for the period April 1981 to March 1983. The characteristics of the long waves and the relation between the long- and short-period wave heights are described in Botes, Russell and Huizinga (1983). The long-period wave heights between 50 s and 110 s measured in the Koeberg basin are illustrated in Figure 2 where the wave height exceedance curves are drawn for the three recording positions.

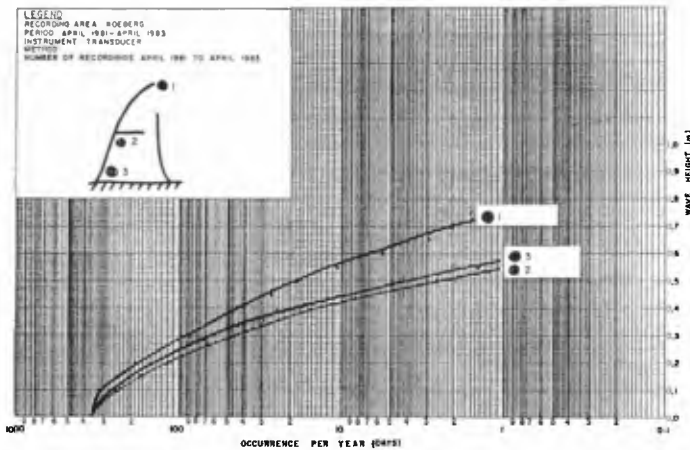


Figure 2. Long-period wave height exceedances

The analysis of the data was based on the auto-covariance method and is described in Botes (1980).

3. THE NUMERICAL MODEL

3.1 General

The computations for this numerical model were based on the approximation of the hydrodynamic equations (conservation of mass and momentum equations in terms of the water elevation and depth average velocity) by using finite-difference techniques. The finite-difference modelling scheme, originally developed by Leendertse (1967), was adapted at the CSIR to accommodate any harbour layout (Russell and Huizinga, 1978). The modifications included radiative open boundaries, based on the method of characteristics which could be applied to any of the model boundaries to permit the passage of reflected waves. The same type of boundary was constructed on the side of the model which faced the main long-wave direction for the input wave conditions.

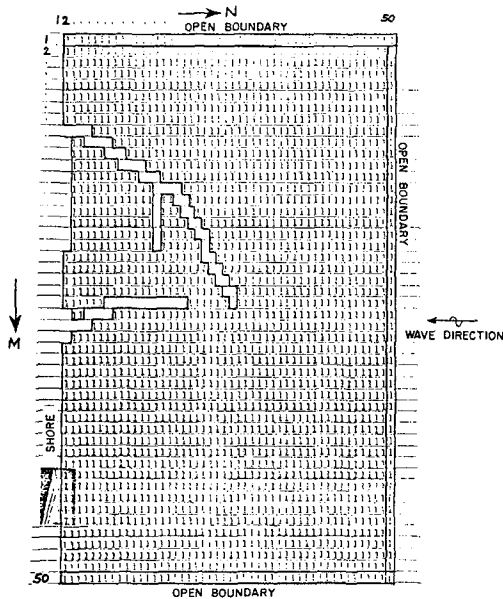


Figure 3. Computational field of the numerical model

The model area of Koeberg was represented by a two-dimensional grid system (50×50) with a grid size of 30 m which was the largest grid size which could describe this particular harbour configuration accurately.

At each grid point the depth and bottom friction were described and the velocities and water level fluctuations were calculated.

The computational field of the model was described by a notation of "1"'s and "0"'s with which the harbour configuration, shoreline, boundaries, etc. could be defined. The model created a computational notation by scanning this field vertically and horizontally. The computational field is described in Figure 3.

3.2 Input Conditions and Output of the Model

A method was developed to incorporate a range of frequencies in one model run by simulating an input wave spectrum which could be obtained by the bandpass filtering of a white noise spectrum. During the model run, time-series recordings were made at selected grid locations. These time-series were analysed in the frequency domain and the amplifications between two locations were obtained by the direct relation between the spectral density estimates of the two selected locations. The analysis was based on the auto-covariance method and is described by Botes (1983).

The advantages of this method were that the model and prototype data could be compared directly for calibration purposes and that it led to impressive savings over an approach where individual regular long waves were used in the model.

Frequencies which caused high amplifications were identified and the model was then operated with a sine wave input, with frequencies similar to the identified peaks. Maximum water level fluctuations over the entire harbour area were obtained as well as velocity vector fields at certain time steps.

3.3 Selection of Grid Size and Time Step

The computational time and cost of such a numerical model is directly related to the grid size and the computational time step.

The grid size must be small enough to provide not only a sufficient description of the coastline and harbour geometry but also to describe the bottom topography accurately. Bottom profiles can be very irregular with deep, narrow channels as at the entrance of the Koeberg basin. For adequate description of the Koeberg basin a maximum grid size of 30 m was needed for this study.

The computational system is unconditionally stable and is consistent so that the solution of the difference equations converge to the solution of the differential equations, the "true solution", as the grid size and time-step approach zero.

The stability, convergency and accuracy of the scheme is described by Leendertse (1967). The computational time-step can be determined theoretically with a few guidelines such as the Courant criterion and wave description, for the minimum phase and amplitude deformation. However, there was still a need to determine the sensitivity of the model compared to prototype measurements. If various layouts for a harbour are to be tested for a preliminary study, considerable cost can be saved if a bigger time-step than that theoretically decided on, can be used as long as the results are within acceptable limits.

The accuracy of the model (amplitude) compared to prototype responses for various time steps was determined with this series of tests.

4. RESULTS

4.1 Calibration

As mentioned, the grid size is controlled by the harbour geometry and topography. Initially a grid size of 30 m was chosen. For an average depth of 7 m the wave celerity is:

$$C = \sqrt{gd} = 8,29 \text{ m/s}$$

where d = depth (m)
 g = gravitational acceleration (m/s^2).

For the best first approximation to a value for Δt we can put the Courant number, C_T , equal to 1:

$$C_T = C \cdot \Delta t / \Delta l = 1$$

where Δl = model grid size (m)
 Δt = model time step (s).

For $C = 8,29$ and $\Delta l = 30$

$$\Delta t = \frac{30}{8,29} \approx 3,62$$

$$\Delta \tau = 4,0 \text{ s.}$$

With a time step of 4,0 s and a grid size of 30 m the model was run with a random input between 0,0075 Hz (133,3 s) and 0,026 Hz (38,5 s). For the shortest wave, that is 38,5 s, the wave description (number of points per wave length) was $T/\Delta t = 9,6$ and $L/\Delta l = 10,6$, which according to Leendertse (1967) is approximately the lower limit for wave description before considerable phase shift will occur.

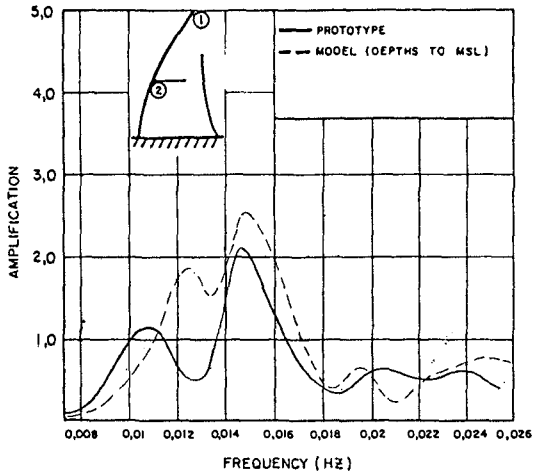


Figure 4. Prototype and model responses for $\Delta t = 4,0$ s

The model responses between locations 1 and 2 are compared to the prototype data in Figure 4. The model topography was similar to the prototype topography that existed when the long waves were recorded.

The peak amplification at 0,015 Hz (66,67 s) compared well with the prototype data. This is the standing wave between the lateral arm and the shore side of the basin. Although the form of the total response wave tended to the shape of the prototype response curve, the correlation became worse from 0,013 Hz and lower. This is due to the lack of exact description of the topography in the outer basin which was still in the construction stage (dredging) during the time when the prototype data were recorded.

During 1978 an existing physical short-wave penetration model (scale 1:80) was used to investigate the response of the physical model to long waves.

This physical model had been constructed with a simplified harbour topography (a depth of 6,0 m throughout) and responded to a wave of 91 s. The numerical model responded to a wave of 85 s when an average depth of 6,0 m was also used in the model.

The resemblance between the velocity fields of the numerical and physical models is illustrated in Figure 5.

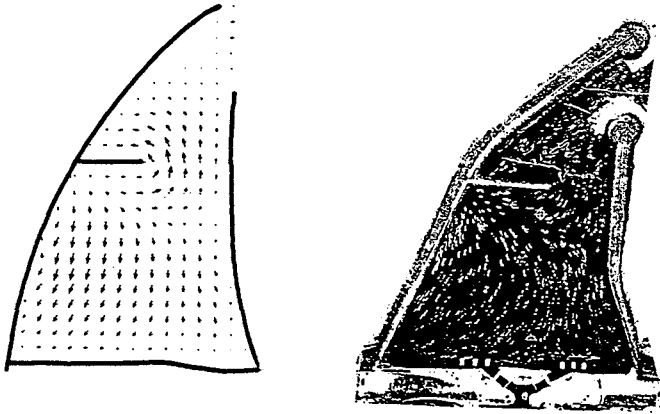


Figure 5. Velocity fields

Numerical model
 $T = 85,7$ s

Physical model
 $T = 91,0$ s

4.2 Influence of Varying Time-steps on the Accuracy of the Model

As the grid size was fixed for the description of the layout it was attempted to increase the computational time-step in order to economize the model.

Although the shape of the response curve changed with a bigger time-step the peak response period and the magnitude of the amplification for the basin remained the same for a computational time-step of 6,0 s which resulted in a $T/\Delta t$ of 6,4 and Courant number of 1,7. The result is illustrated in Figure 6.

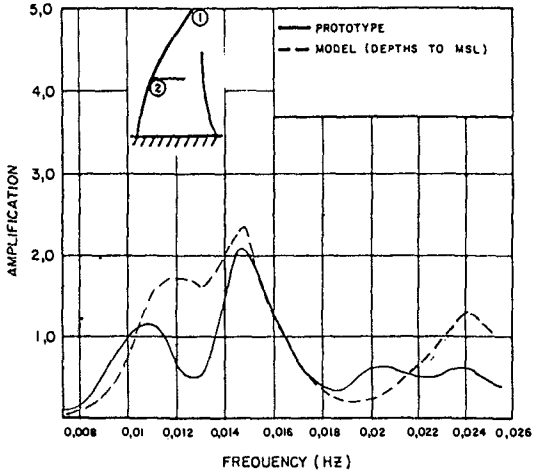


Figure 6. Prototype and model responses for $\Delta t = 6,0$ s

The influence of the time-step on the accuracy of the model is best illustrated when the amplifications and velocity fields over the entire harbour area for the peak period of 66,67 s are compared as illustrated in Figures 7a-f.

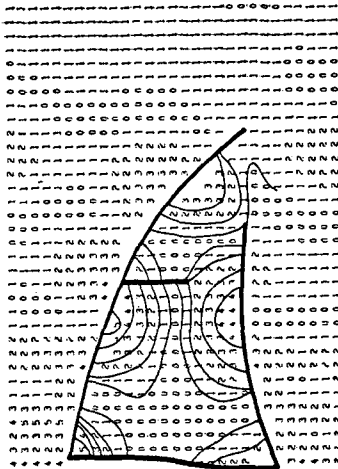


Figure 7a. Maximum amplifications
 $\Delta t = 4,0$ s,
 $T = 66,7$ s,
 Input height = 0,1 m

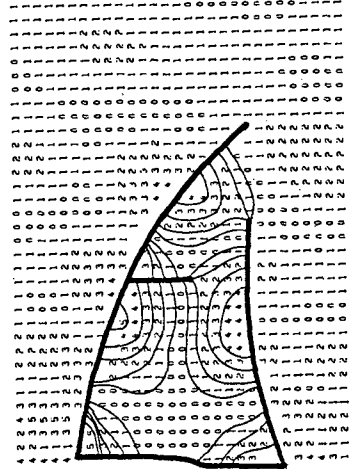


Figure 7b. Maximum amplifications
 $\Delta t = 6,0$ s,
 $T = 66,67$ s,
 Input height = 0,1 m

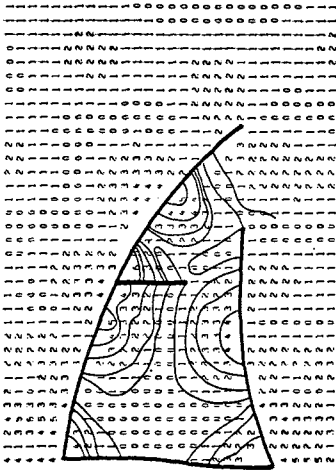


Figure 7c. Maximum amplifications
 $\Delta t = 8,0$ s,
 $T = 66,67$ s,
 Input height = 0,1 m

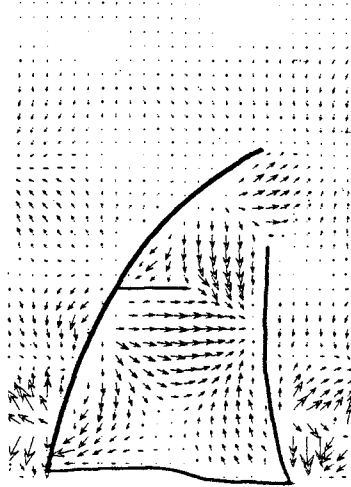


Figure 7d. Velocity field
 $\Delta t = 4,0$ s,
 $T = 66,67$ s,
 Input height = 0,1 m

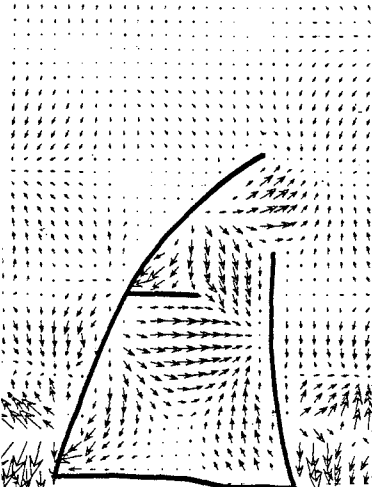


Figure 7e. Velocity field
 $\Delta t = 6,0$ s,
 $T = 66,7$ s,
 Input height = 0,1 m

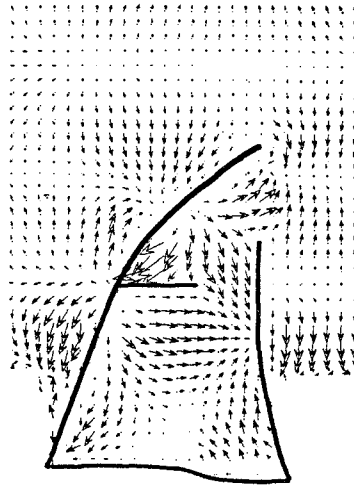


Figure 7f. Velocity field
 $\Delta t = 8,0$ s,
 $T = 66,7$ s,
 Input height = 0,1 m

From these figures it can be seen that a computational time-step of 8,0 s ($T/\Delta t = 4,81$, Courant number = 2,2), which is twice the theoretically determined time-step, can still be used when numerous preliminary tests are necessary to determine an optimum layout. This results in considerable savings on computer cost and time.

However, for a time step of 10,0 s ($T/\Delta t = 3,85$, Courant number = 3,0). As shown in Figure 8, there is no sign of the characteristic response of the basin when compared to Figures 7a-c.

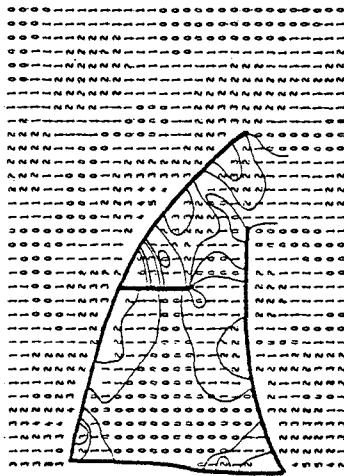


Figure 8. Maximum amplifications

4.3 Influence of the Magnitude of the Input Wave

As the long-wave amplitudes range between 10 and 50 cm in the prototype, the influence of the magnitude of the input waves to the model was investigated.

As experienced with the prototype data the model response was consistent, irrespective of the magnitude of the input waves as illustrated in Figure 9 and compared to Figure 7b.

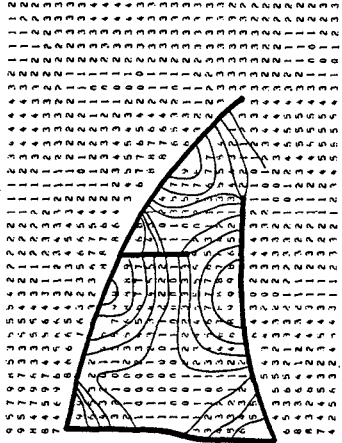


Figure 9. Maximum amplifications
 $\Delta t = 6,0 \text{ s}$, $T = 66,7 \text{ s}$,
 Input height = $0,2 \text{ m}$
 Amplifications are the values divided by 2

4.4 Influence of Water Depth

In relatively shallow areas in a harbour layout the water levels are of great importance when comparing model results to prototype data as illustrated in Figure 10 where the responses of the model for water levels at spring, mean and neap tides are compared with prototype data.

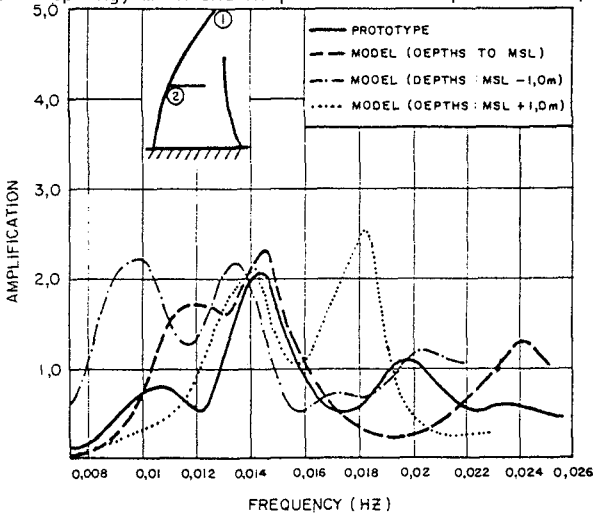


Figure 10 Model responses at different water levels compared to prototype data

5. CONCLUSIONS

- (1) The prototype data provided valuable information on wave-height exceedances, correlation between short and long-period wave heights, and response data to calibrate and verify the numerical model.
- (2) The numerical model could be calibrated with a computational time-step of 4,0 s.
- (3) Resemblance between the physical and numerical model results is very good.
- (4) For basic investigations with the response frequency, larger time-steps can be used in order to save cost and time.
- (5) For a wave description ($T/\Delta t$) $< 4,8$ and a Courant number $> 2,2$ the model results are completely inaccurate.
- (6) In relatively shallow harbours the response of the basin is strongly influenced by the water depths (tidal variation).
- (7) The response of a basin (i.e. pattern of oscillation and degree of amplification) is not influenced by the magnitude of the input wave height.

REFERENCES

- BOTES, W A M (1980). Application of digital time series analysis to a resonance study at Table Bay Harbour. CSIR Report SEA 8006.
- BOTES, W A M, RUSSELL, K S and HUIZINGA, P (1982). Resonance in South African harbours. Proceedings ICCE 1982, Cape Town.
- LEENDERTSE, J J (1967). Aspects of a computational model for long period water wave propagation. The Rand Corporation, RM-5894-PR.
- RUSSELL, K S and HUIZINGA, P (1978). A two-dimensional finite-difference numerical model for the investigation of harbour resonance. CSIR Report IR 7804.